

Influence of the filament potential wave form on the sensitivity of glass-envelope Bayard-Alpert gages

Patrick J. Abbott and J. Patrick Looney

Thermophysics Division, Chemical Science and Technology Laboratory, National Institute of Standards and Technology, Gaithersburg, Maryland 20899

(Received 5 May 1994; accepted 15 June 1994)

Nonlinearities of ~10%–15% in the sensitivity of glass envelope Bayard-Alpert gages (BA gages) have been observed in the pressure range 10^{-7} – 10^{-2} Pa. These nonlinearities were studied in modified BA gage tubes with platinum coatings on their inner glass surfaces by measuring the equilibrium potential of the platinum coating as a function of pressure. The sensitivities of the gage systems (gage tube plus controller) were found to depend on the inner surface potential, and this potential was found to depend on pressure and on the details of the filament potential waveform provided by the gage controller. It was found that the nonlinearities could be minimized by holding the inner surface to a fixed direct-current (dc) potential, by modifying the alternating-current filament potential wave form, or by using a controller that provides a noise-free dc filament-heating current.

I. INTRODUCTION

The NIST Vacuum Group calibrates ionization gages between 10^{-7} and 10^{-1} Pa (10^{-9} and 10^{-3} Torr) to be used as vacuum reference standards in industrial and government laboratories. Most of the gage systems consist of a glass envelope Bayard-Alpert (BA) gage tube and an electronic control unit which are calibrated together as a system, since the overall response is a combination of the behavior of both the gage tube and the controller. A typical calibration consists of measuring the response of the gage system as a function of pressure for a particular gas, most often nitrogen, for a given set of operating parameters. In many cases, the calibration results for these gage systems exhibit pressure dependencies, or nonlinearities, that significantly exceed those attributable to the gage tube alone. Some of the nonlinearities can be explained by imperfections in the controllers, e.g., a nonlinear response of the ion current measuring circuit. However, for many gage systems the explanation is not so evident. We have observed that glass-envelope gage systems often exhibit a nonlinear response to pressure of between 5% and 15%. Two examples of this behavior are shown in Fig. 1. For a particular gage system the response is usually very stable, and although nonlinear, the response will repeat to within a few percent, even when recalibrated over a period of a year or more. Additionally, the electrical performance of the controllers is quite satisfactory. Typically, these controllers provide bias voltages that are maintained to within 1 V, emission currents that are constant to within 1%, and ion current measuring circuitry that is linear to within a few percent over the operating range. As a further check we have repeated some calibrations, substituting calibrated picoammeters in place of the controller's ion current measuring circuit, and have found similar overall nonlinear results. Continued observation of these nonlinearities over several years and for many different glass-envelope BA gage systems prompted us to further examine this effect. In this article we show that these nonlinearities are due to a pressure-dependent charging of the glass tube, which is caused by a

changing filament potential associated with the use of chopped alternating-current (ac) filament-heating current wave forms. We also show several ways in which this effect can be minimized or eliminated.

II. GAGE SENSITIVITY

BA ionization gages are the most widely used total pressure gages in the high and ultrahigh vacuum regimes (10^{-8} – 10^{-1} Pa). Their operation, discussed in detail elsewhere,¹ relies on the ionization by electron bombardment of gas molecules within the gage structure and the measurement of the positive ion current produced by this process. If the electron emission current and the temperature of the gas are constant, then the ion current is proportional to the number density or the pressure of the gas within the gage over a large range of pressures. This implies that the sensitivity of the gage S' is constant, and can be related to the pressure P , the emission current I^e , and the collector current I^+ through the following relation:²

$$S' = \frac{I^+ - I_r}{I^e P}.$$

In this equation, I_r is a pressure-independent residual current. An ion current measuring circuit within the controller is used to convert the collector current into an analog or digital pressure indication. The gage "tube" is available from a number of suppliers in two configurations: nude, in which the structure is mounted on a metal flange and inserted directly into the vacuum chamber, and glass-enclosed, in which the structure is enclosed by a glass envelope. The present discussion applies only to the glass envelope variety.

Since the invention of the BA gage in 1950, there have been many investigations of the factors that affect the gage's sensitivity. In particular, several researchers have shown that the sensitivity of a BA gage tube can be influenced significantly by its electrical boundary conditions. Carter and Leck³ attributed their observation of bistable behavior of BA gages to the charging of the inner surfaces of the gage tube as a

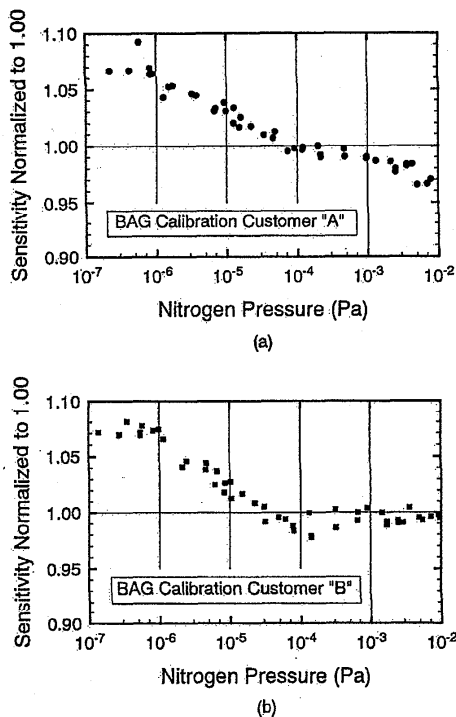


FIG. 1. Sensitivity vs pressure calibration results for two customer-owned, glass-envelope BA gage systems. The gages were operated with different controllers that provided the same nominal operating parameters ($V_{fil}=+30$ V, $V_{grid}=+180$ V, $I_e=1$ mA).

result of secondary emission processes. To overcome the instability, they recommended that an equipotential surface of low secondary emission be deposited upon the glass walls. This finding is presumably the basis for the platinum-coated gage tubes that are available today. Redhead,⁴ using a glass-envelope gage with a transparent conductive coating of tin oxide on the inside surface, found that the sensitivity of the gage varied as a function of the potential on the inner surface for a given filament-to-grid spacing.

Expanding on Redhead's work by using computer simulations, Pittaway⁵ related changes in sensitivity to the paths taken by ionizing electrons as a function of grid-to-screen (inner glass surface) potential. In this laboratory, McCulloh and Tilford⁶ observed that the sensitivity of a nude BA gage housed in a grounded stainless-steel tube was 15% greater than when it was mounted nude in the gage port. Furthermore, Tilford, McCulloh, and Woong,⁷ working with broad range ionization gage tubes, observed that when the shield (platinum coating on the inner glass surface) of one gage, normally held at 0 V, was allowed to float up to filament potential, the collector current increased by 23%. These works are in agreement with our observation that a pressure-dependent potential on the inner surface of a glass-envelope BA gage causes the sensitivity nonlinearities that we have encountered.

There is no evidence to suggest that the primary standard

used to perform the calibrations (discussed below) is systematically introducing errors that would account for the nonlinear sensitivities that have been observed. Furthermore, not all gage system calibrations exhibit nonlinearities. Using the same primary standard, Filippelli and Dittmann⁸ found that for a variety of hot-cathode gages, consisting primarily of nude BA and extractor gages operated with NIST-built controllers, the sensitivity response for N_2 was constant to within a scatter of $\pm 3\%$ over the range 1×10^{-7} – 2×10^{-3} Pa.

III. EXPERIMENT

The NIST primary ultrahigh vacuum standard^{9–11} was used to calibrate two nominally identical BA gages obtained from the same supplier and modified for this study as discussed below. All quoted uncertainties represent the two-standard deviation (2σ) values. The primary standard uses the orifice-flow technique to generate calibration pressures by measuring the amount of gas that flows through an orifice whose conductance is accurately known. The orifice flow technique was used to generate pressures between 10^{-7} and 10^{-4} Pa; for pressures greater than 10^{-4} Pa, calibrated spinning rotor gages were used to measure the pressure. The systematic uncertainties range from $\sim 2.6\%$ at 10^{-7} Pa to 0.9% at 10^{-1} Pa. Prior to this study, the chamber was baked under vacuum for ~ 8 h at $\sim 270^\circ\text{C}$. This produced a base pressure of about 1×10^{-8} Pa as indicated by an extractor gage. The filaments of the BA gages used in this study were operated during the bake to degas the devices. No further degassing procedures were employed. Except for brief interruptions, all of the gages were operated continuously throughout the study. Calibration data were taken over several days, with nitrogen as the calibration gas.

The test BA gages, designated BAG #1 and BAG #2, were attached to the standard with copper-gasketed high-vacuum flanges. As received from the supplier, the gage tubes were equipped with a single, thoriated iridium (ThO–Ir) filament, and an internal platinum coating on the glass envelope. Both gages were modified so that the platinum coating could float electrically or be held at a direct-current (dc) potential independent of other gage electrodes. A diagram of the modified BA gage tubes is shown in Fig. 2. The platinum coating will be referred to as the "shield" electrode. BAG #1 and BAG #2 were operated with commercial controllers from different manufacturers, designated controller #1 and controller #2, that are typical of units that are widely used, and for which we have previously observed nonlinearities. The operating parameters for each of the gage systems are shown in Table I below. The uncertainty on each of the measured quantities is less than 0.5%.

Digital picoammeters were used to measure the collector currents of BAG #1 and BAG #2 as a function of the nitrogen pressure generated by the standard over the pressure range 10^{-7} – 10^{-2} Pa. The uncertainty of the picoammeters ranged from $\pm 0.5\%$ at the lowest measured ion currents to $\pm 0.1\%$ for ion currents corresponding to the highest calibration pressures. At each pressure, two collector current readings were recorded: with the shield fixed to +30 V dc and with the shield electrically floating. The equilibrium potentials on the shield electrode for the "floating" conditions

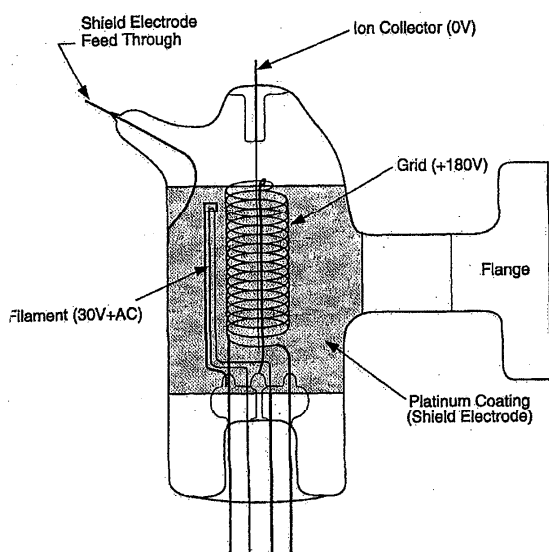


FIG. 2. Diagram illustrating the modified BA gage tubes used in this study. Nominal operating potentials for each electrode are shown. The shield electrode can float or be held at a fixed potential. The filament potential is a chopped-ac wave form biased by a +30 V dc potential.

were also recorded at each pressure. The shield-to-ground resistance was determined experimentally to be $\sim 10^9 \Omega$, so the floating shield potentials were measured with dc voltmeters that had a larger input impedance, on the order of $10^{14} \Omega$. The floating shield potential was actually periodic in response to the chopped ac filament potential (discussed in a later section), and was, in effect, "averaged" by the dc voltmeters. Based on the repeatability of the shield potential measurements, we calculated the uncertainty of these measurements to be ~ 1 V. The uncertainty of the voltmeters was less than $\pm 0.05\%$ for dc potential measurements. All reported sensitivities were corrected for base pressure conditions.

IV. RESULTS

The results of the N_2 sensitivity measurements are shown in Figs. 3(a) and 3(b), normalized to 1.00 at 10^{-4} Pa for the floating shield condition. These figures show several interesting features. The sensitivities with the shield held at 30 V dc for both gages varied by less than 3% over the calibration pressure range. However, the sensitivities with the shield potential floating were pressure-dependent over the calibration pressure range for both gage systems, but did not change in

TABLE I. Operating parameters for the experimental BA gage systems.

Gage system	Grid bias (V dc)	Filament bias (V dc)	Emission current (mA dc)
BAG #1+controller #1	+180.2	+30.20	0.990
BAG #2+controller #2	+180.8	+29.68	1.000

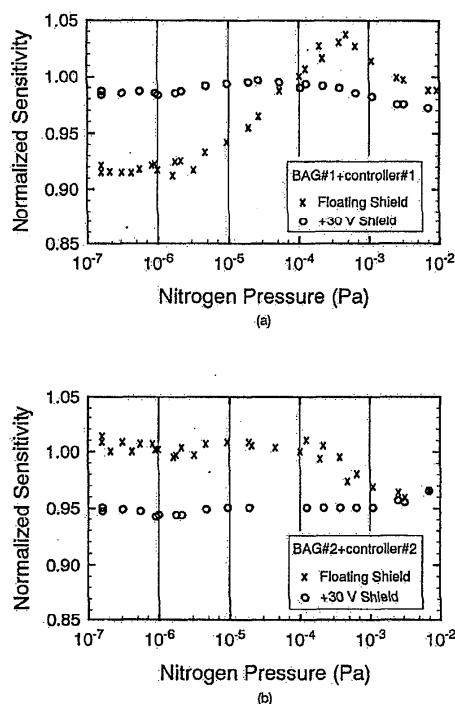


FIG. 3. Normalized sensitivity vs pressure calibration results for the test BA gage systems. The sensitivities for each gage system have been normalized to 1.00 at 10^{-4} Pa for the floating shield condition. Results for BA gage system (BAG #1+controller #1) are shown in (a) and those for (BAG #2+controller #2) are shown in (b).

the same direction or by the same amount. For BAG #1, the difference between maximum and minimum sensitivity was $\sim 11\%$, and for BAG #2 it was $\sim 5\%$. These results are typical of our experience.

The floating shield potentials were measured with respect to ground and are shown as a function of pressure in Fig. 4. These data indicate that both gage tubes exhibited a pressure-dependent charging of the inner surface of the glass envelope. Note that the curves have a similar shape, and even overlap at higher pressures, but that the potentials at the low-

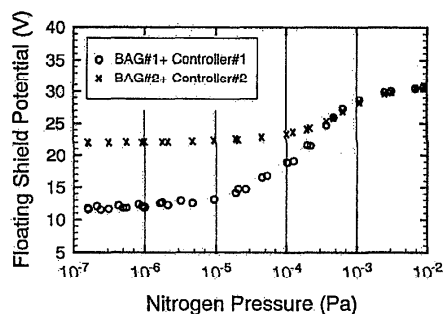


FIG. 4. Floating shield potential vs pressure for the test BA gage systems.

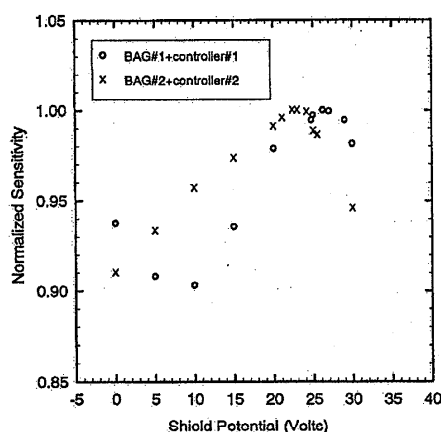


Fig. 5. Sensitivity vs shield potential at a pressure of 4.8×10^{-4} Pa of N_2 for the test BA gage systems.

est pressures differ greatly. Note further that the slope of each curve in Fig. 4 is greatest between 10^{-4} and 10^{-3} Pa, and that both curves have a maximum value of ~ 31 V dc.

To determine the effect of the pressure-dependent floating shield potential on sensitivity, we measured the sensitivity of each gage system as a function of the shield potential at a constant pressure. Data taken at a pressure of 4.8×10^{-4} Pa are shown in Fig. 5. This figure illustrates that the sensitivity of each gage changes by nearly 10% when the shield potentials are changed from 0 to 30 V. Furthermore, sensitivity maxima occur at 27 V for BAG #1 and 22.5 V for BAG #2, and a sensitivity minimum occurs for BAG #1 at a shield potential of +10 V. To gain further insight, we also examined the filament-heating current provided to the gage tubes by their respective controllers. These controllers heat the gage filaments with a chopped-ac wave form that is superimposed on a dc bias potential. This wave form is applied to one of the filament posts, the "high" potential post, and current flows through the filament to maintain the proper emission temperature only during the ac voltage excursions, the duty cycle being determined by a feedback circuit that regulates the electron current that leaves the filament. The filament-heating wave forms provided by controller #1 and controller #2 were measured at the high potential filament posts with respect to ground for a pressure of 10^{-6} Pa and are shown in Figs. 6(a) and 6(b), respectively. Note that the wave forms are similar except that the waveform used to heat BAG #1 [Fig. 6(a)] shows a series of oscillations, or spikes, at the start of each ac excursion and for $\sim 40 \mu\text{s}$ thereafter. The lowest potential point on this waveform is ~ 13 V for a dc bias potential of 30 V; in contrast, the lowest potential point on the BAG #2 filament-heating wave form [Fig. 6(b)] is ~ 19 V. The spikes on the filament potential of BAG #1 were found to originate in the bias supply circuitry and were seen only when the filament potential was measured with respect to ground; when the potential was measured across the filament, the spikes were absent, but the wave form was otherwise unaffected.

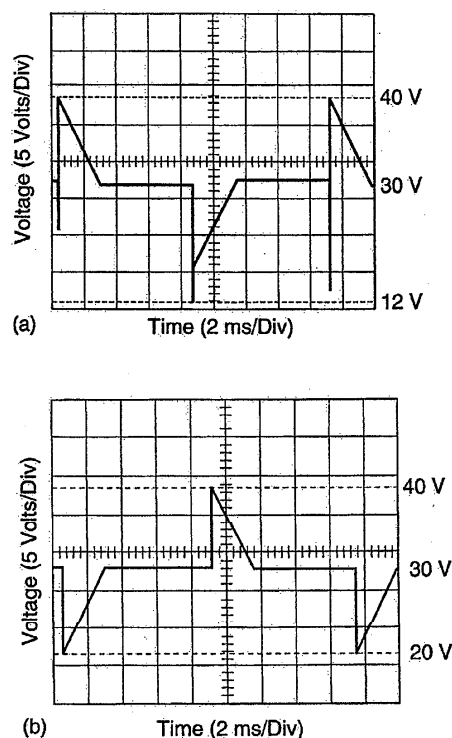


Fig. 6. Filament potential wave forms for the test BA gage systems, measured with respect to ground. The wave form for gage system (BAG #1 +controller #1) is shown in (a) and that for gage system (BAG #2 +controller #2) is shown in (b).

Two interesting features of the behavior of the test BA gage systems are observed by comparing Figs. 4 and 6. These figures show that the BAG #1 low-pressure floating-shield potential is significantly lower than that of BAG #2, and that the filament-heating wave form for BAG #1 has a correspondingly lower minimum potential than the wave form for BAG #2. Subsequently, measurements were performed to determine if a correlation existed between the minimum filament potential and the low-pressure shield potential for each gage system. It was possible to vary the amplitude of the spikes on the filament-heating wave form of BAG #1, and thus the minimum filament potential, by inserting a filtering capacitor between the high potential filament post and ground. Using capacitors of increasing size, we reduced the spikes' amplitude to as small as 1 V. At a pressure of 10^{-8} Pa, this increased the minimum potential on the wave form from 11 to 20 V. In response the shield potential rose from 12 to 22 V, the same shield potential observed for BAG #2 at this pressure. Closer examination revealed that at the lowest pressures, the changes in the floating shield potential tracked on a 1:1 basis with the corresponding changes in the minimum filament potential. Similar results were obtained for BAG #2.

The results of these measurements show that the sensitivities of the experimental BA gage systems are dependent on the shield potential. A fixed shield potential yields a constant

sensitivity, however the floating shield potential is pressure dependent and does not have the same functional form from one gage system to another. These findings explain the pressure-dependent sensitivities that have been observed for glass-envelope BA gage systems. One may calculate the shapes of the sensitivity versus pressure curves for the floating shield condition (Fig. 3) by combining the floating potential versus pressure curves (Fig. 4) and the sensitivity versus shield potential curves (Fig. 5). Therefore, the key to explaining the nonlinear response of BA gage systems is the pressure dependence of the shield potential. But why does the shield potential change as a function of pressure in the first place?

A simple analysis of the electron and ion optics within the gage tube can show that the pressure-dependent shield potential is due to the balance between the electron and ion currents going to the shield. Electrons produced at the filament are accelerated toward the grid. Most of the electrons then oscillate in and out of the volume defined by the inside of the grid, creating ions, until they are collected by the grid electrode. Ionization of gas molecules within the grid volume creates an ion current at the collector that varies from picoamps to microamps as the pressure increases from 10^{-8} to 0.1 Pa. Ionization outside of the grid volume creates a comparable number of ions that are accelerated to the shield by the large grid potential. This ion current increases the potential of the shield with a time constant that depends on the capacitance between the shield and ground.¹²

An electron that passes through the grid volume has a kinetic energy determined by the difference between the grid potential and the potential of the filament at the time and the place the electron was emitted. Let us call this filament potential V_0 . If V_0 is less than the shield potential, then it is energetically possible for the electron to reach the shield. As the shield collects electrons, its net charge is lowered. When the shield has collected enough electrons so that its potential has been reduced to V_0 , electrons emitted at potential V_0 can just reach the shield, and an equilibrium then exists between the ion and electron currents to the shield. This equilibrium establishes the shield's potential for a given pressure. It is instructive to apply this reasoning to the test BA gages. At low pressures, where the ion current is many orders of magnitude less than the electron emission current, the electrons emitted during the short negative-going spike seen in Fig. 6(a) (BAG #1) are enough to neutralize the ions accumulated on the shield during the entire previous heating current cycle. This effectively fixes the shield potential at the minimum filament potential over several decades of pressure, as seen in Fig. 4. As the pressure and ion current increase, the electrons produced at the minimum filament potential are no longer sufficient to neutralize all of the positive charge accumulated on the shield during the previous heating current cycle, so the ion current charges the shield to a higher potential, averaged over a heating current cycle. This dynamic balance between the electron and ion currents collected by the shield continues throughout the operating pressure range of the gage tube, with the *average* shield potential changing to reflect the relative abundance of incoming positive and negative charge. The detailed shapes of the curves in Fig. 4 will

depend on the filament potential wave form shown in Fig. 6 as well as the electrode spacing, but for each gage, the low pressure shield potential is determined by the *minimum* filament potential. This interpretation is complicated by the pressure-dependent filament-heating power, resistive voltage gradients along the filament, field perturbations between the grid and shield, space-charge effects at higher pressures, and the ac nature of the filament potential. Work is in progress to determine the effects of the ac filament potential on gage behavior more accurately, but preliminary results indicate that the dc shield potential measurements made in this study provide a reasonably good time average of the actual shield potentials. Therefore, the above discussion does provide a qualitative explanation for the data in Fig. 4.

An interesting aspect of the sensitivity variation with shield potential is that different gage tubes of nominally identical geometry can be made to have the same sensitivity at a given pressure by adjusting the shield potential on each gage tube. Furthermore, measurements made using the two modified BA gages showed that the difference in the sensitivities for the two gages was less than 2% over the pressure range 10^{-6} – 10^{-2} Pa when the shield potentials had been chosen to yield equal sensitivities at 10^{-3} Pa. This property would be useful for systems using more than one BA gage.

Several approaches to minimize the pressure dependence of the sensitivity were investigated. The data presented in Fig. 3 show that by maintaining the shield potential at a constant value, the sensitivity remains constant, thereby eliminating the deleterious effects of time-varying filament potential. However, the majority of BA gage tubes in use does not have a conductive coating on the glass envelope to facilitate the application of a constant potential.

The problem can also be effectively eliminated by using a controller that provides a noise-free dc filament-heating current. For this type of controller, there is a potential difference across the filament that varies from 3 to 4 V with pressure, and the glass envelope will charge to an intermediate value that varies by less than 4 V over the operating pressure range, with a correspondingly small sensitivity variation. We have used NIST-made controllers of this type for many years and have never observed nonlinearities of the type discussed in this article. However, even with dc filament power, one must be careful to ensure that the filament current is truly noise-free. We have experience with one type of commercial "dc" controller whose filament bias potential contained 50 kHz "spikes" with a peak-to-peak amplitude of ~ 30 V. The spikes were found to affect the gage performance in the same manner as the high frequency oscillations on the filament-heating current wave form for BAG #1. In this case, the shield potential was ~ 15 V at 10^{-5} Pa and tracked on a 1:1 basis with changes in the minimum potential of the filament which were produced by adding filtering capacitors. The spikes were presumably caused by leakage from the controller's high-frequency switching power-supply circuit.

Since the changing shield potential is caused by the negative-going part of the ac filament-heating current, another way to stabilize the shield potential is to insert a diode in series with the filament to eliminate the negative-going half-cycle of the chopped-ac wave form. This limits the

minimum filament potential to the dc bias potential minus the small drop across the diode (~ 1 V). We experimented with this approach using BAG #1 and controller #1, and found that the shield potential changed by only 3 V over the pressure range 10^{-5} – 10^{-1} Pa. The corresponding sensitivity was not measured, but the data in Fig. 5 indicates that the sensitivity should not change by more than a few percent. The controller responded to the diode by increasing the duty cycle of the chopped-ac wave form to maintain the emission current at its preset value. Note that this approach will not prevent the glass envelope from charging to potentials that are higher than the filament bias. This may occur at the highest operating pressures, e.g., 10^{-1} Pa.

V. CONCLUSIONS

We have shown that a pressure-dependent sensitivity is observed with glass envelope BA gage systems and is caused by a pressure-dependent potential on the inner surface of the glass envelope. This pressure-dependent potential is primarily a result of the use of ac filament-heating current. We conclude that all electrically floating glass-envelope BA gage systems that use "ac" controllers will exhibit a pressure-dependent sensitivity. The extent of the nonlinearity is dependent on the range of potentials to which the glass envelope charges as a function of pressure, which is determined by the amplitude and duration of the negative going parts of the filament potential wave form. It was found that this nonlinearity can be minimized by holding the glass envelope at a constant dc potential, by using a controller that provides a noise-free dc filament-heating current, or by eliminating negative-going ac excursions on the filament potential wave form.

ACKNOWLEDGMENTS

The authors would like to thank our colleagues in the NIST Vacuum Group, especially Charles Tilford for reading

this manuscript and offering many useful suggestions, and Fred Long for electronics support and numerous discussions involving the behavior of BA ionization gage controllers. They also thank Jeffrey R. Anderson for his work in modifying the BA gages used in this study. The authors would also like to gratefully acknowledge P. A. Redhead of the National Research Council of Canada for reading this manuscript and providing many useful comments.

¹R. T. Bayard and D. A. Alpert, *Rev. Sci. Instrum.* **21**, 571 (1950); see also recent texts on vacuum technology.

²See, for example, J. F. O'Hanlon, *A User's Guide to Vacuum Technology*, 2nd ed. (Wiley, New York, 1989), p. 90.

³G. Carter and J. H. Leck, *B. J. Appl. Phys.* **10**, 364 (1959).

⁴P. A. Redhead, *J. Vac. Sci. Technol.* **6**, 848 (1969).

⁵L. G. Pittaway, *J. Phys. D: Appl. Phys.* **3**, 1113 (1970).

⁶K. E. McCulloh and C. R. Tilford, *J. Vac. Sci. Technol.* **18**, 994 (1981).

⁷C. R. Tilford, K. E. McCulloh, and Han Seung Woong, *J. Vac. Sci. Technol.* **20**, 1140 (1982).

⁸A. R. Filippelli and S. Dittmann, *J. Vac. Sci. Technol. A* **9**, 2757 (1991).

⁹S. Dittmann, *High Vacuum Standard and Its Use*, NIST Special Publication SP 250-34, 1989 (unpublished).

¹⁰C. R. Tilford, S. Dittmann, and K. E. McCulloh, *J. Vac. Sci. Technol. A* **6**, 2853 (1988).

¹¹K. E. McCulloh, C. R. Tilford, C. D. Ehrlich, and F. G. Long, *J. Vac. Sci. Technol. A* **5**, 376 (1987).

¹²In the case of a glass envelope gage tube with a conductive coating on the inner surface, there are two other currents which bear mentioning; first, the secondary electron current due to positive ion impingement on the conductive coating (Auger electrons), and second, the photocurrent of electrons leaving the coating caused by soft x-ray bombardment. The photocurrent is the larger of the two, and may be on the order of 1000 times larger than the photocurrent leaving the collector electrode. Both of these electron currents leaving the coating may be thought of as additional positive ion currents going to the shield, and could be a significant fraction of the shield current at the lowest operating pressures. The authors wish to thank P. A. Redhead of the National Research Council of Canada for kindly bringing these currents to our attention.